Chapter 2

Path Loss Prediction

Today, wireless networks are absolutely ubiquitous and the importance of their role in our daily lives cannot be underestimated. To a large extent, our ability to build and understand these networks hinges on understanding how wireless signals are attenuated over distance in realistic environments. By predicting the attenuation of a radio signal, we can better plan and diagnose networks as well as build futuristic networks that adapt to the spatiotemporal radio environment. For instance, today's network engineers need methods for accurately mapping the extent of coverage of existing and planned networks, yet the efficacy of those approaches is determined by the predictive power of the underlying path loss model (or interpolation regime). Similarly, researchers who investigate dynamic spectrum access networks require accurate radio environment maps to make appropriate and timely frequency allocation decisions, yet the performance of these systems is tied intimately to their ability to make meaningful predictions about the current and future occupancy of the radio channel.

Since the 1940's, researchers and engineers have pondered this problem and have developed myriad schemes that purport to *predict* the value or distribution of signal attenuation (path loss) in many different environments and at different frequencies. This chapter will attempt to give a complete review of the work to date, updating and extending a series of excellent-but-dated surveys from the last 15 years (e.g., [107, 34, 183, 206, 151]).

The first section provides a high-level tutorial on radio propagation, which may be supplemented with either of the excellent surveys by Rappaport [183] and Seybold [206]. After this introduction, the remaining

[0] Work in this chapter has appeared in [175].

sections provide an exhaustive survey of the deep literature available on path loss prediction methods. The chapter concludes with an overview of the state-of-the-art in path loss prediction and coverage mapping methods, including those that use computationally intense ray-optical calculations, and those that utilize some number of measurements to correct predictions. To make sense of all this prior work, these proposals are organized into a new taxonomy for path loss models that groups them into seven major categories and fourteen subcategories. The seven major categories are:

(1) Theoretical/Foundational Models (§2.2.1)

(2) Basic Models (§2.2.2)

(3) Terrain Models (§2.2.3)

(4) Supplementary Models (§2.2.4)

(5) Stochastic Fading Models (§2.2.5)

(6) Many-Ray (Ray-Tracing) Models (§2.2.6)

(7) Active Measurement Models (§2.3)

The discussion here is exhaustive, including more than 50 proposed models from the last 60 years, 30 of which are described in detail. The models are described at a high level with a brief focus on identifying their chief differences from other models. Figure 2.1 provides a family tree of the majority of path loss models discussed in the following subsections and may prove useful for understanding the lineage of various proposals as well as their functional relationship to one another.

The next section provides a brief tutorial on radio propagation. Section 2.2 discusses the bulk of models, which make their predictions *a priori*, without insight from measurements. Section 2.3 discusses models and methods that do use (possibly directed) measurements to inform their predictions. The final sections conclude with a discussion of opportune areas for future work, and motivation for the next chapter, which will seek to understand the practical error of the most popular of these models in realistic environments.

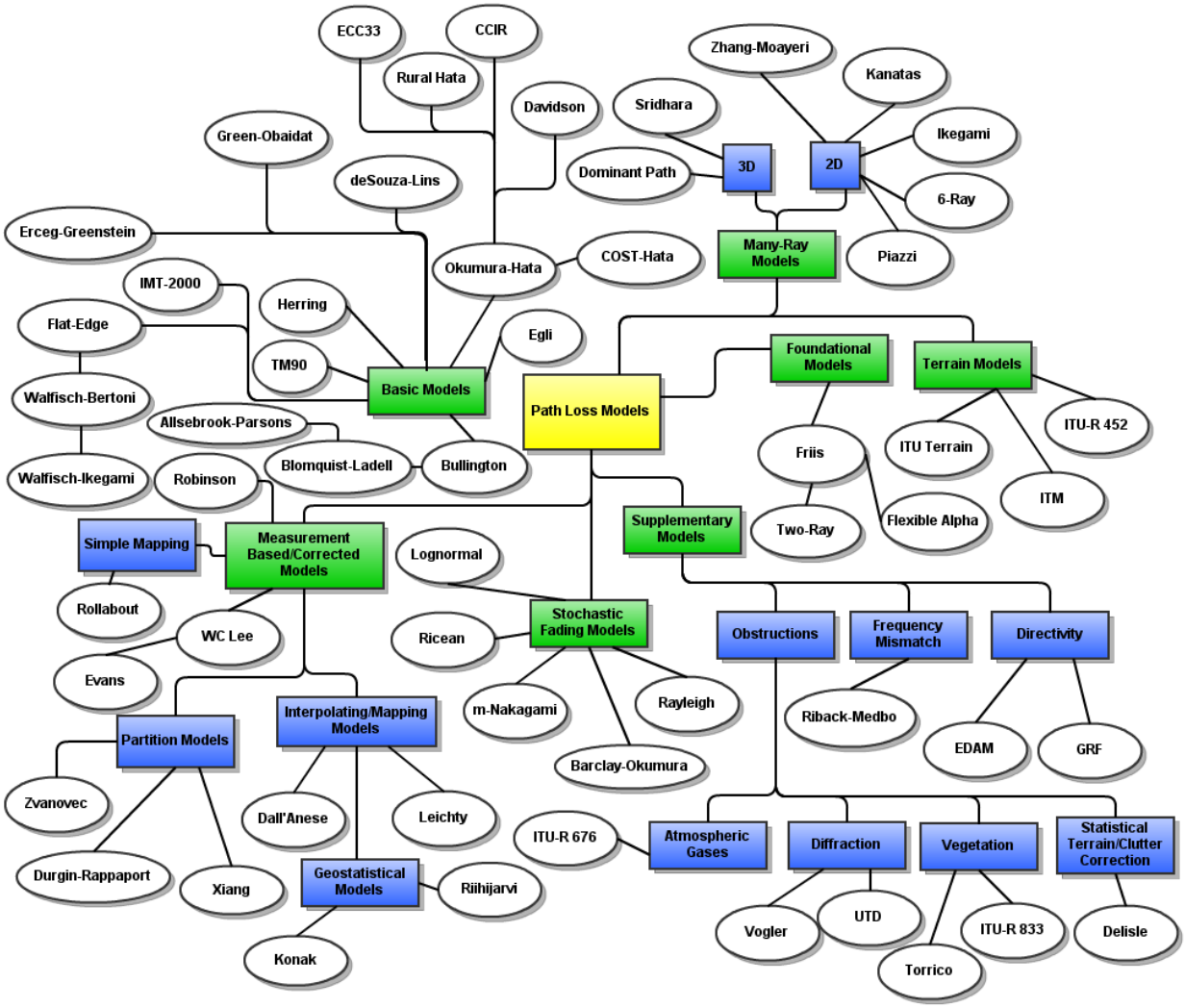

Figure 2.1: Path loss model family tree. Individual models are shown as circles and categories as are shown as rectangles. Major categories are green. Minor categories are blue.

2.1 Radio Propagation Basics

This section introduces the basic concepts of radio propagation. For a more thorough treatment, the intrepid reader can refer to any number of textbooks, including the excellent surveys by Rappaport [183] and Seybold [206].

2.1.1 Signal Propagation

When asked to describe radio, Albert Einstein famously responded:

> You see, wire telegraph is a kind of a very, very long cat. You pull his tail in New York and his head is meowing in Los Angeles. Do you understand this? And radio operates exactly the same way: you send signals here, they receive them there. The only difference is that there is no cat.

The study of radio propagation is largely concerned with what happens in between the head and the tail of the "no cat", so to speak. At each end of the radio link, there is a transceiver that is attached to an antenna of some geometry. The transmitter produces a signal (an electromagnetic plane wave) that is modulated onto the carrier frequency. On its way to the receiver (at roughly the speed of light), the signal reacts with any number of obstacles and then is induced on the receiver's antenna and demodulated. Obstacles in the environment cause the signal to be reflected, refracted, or diffracted, which attenuate the power of the signal (through absorption) and cause scattering and secondary waves. Obstacles that are near the line of sight (LOS) path are said to obstruct the Fresnel zone (technically, the first Fresnel zone's circular aperture) and are most problematic.

In reality it is slightly more complicated than this. Because an antenna radiates its signal simultaneously in all directions, the signal can take many paths to the receiver. Each path may interact with the environment in a chaotically different way and arrive at the receiver delayed by some amount. If these delayed signals are in phase with one another, then they produce constructive interference. If they are out of phase with one another, they produce destructive interference. The spread of this delay is called the *delay spread* and the resulting attenuation is called *multipath fading*. When this attenuation is caused by large

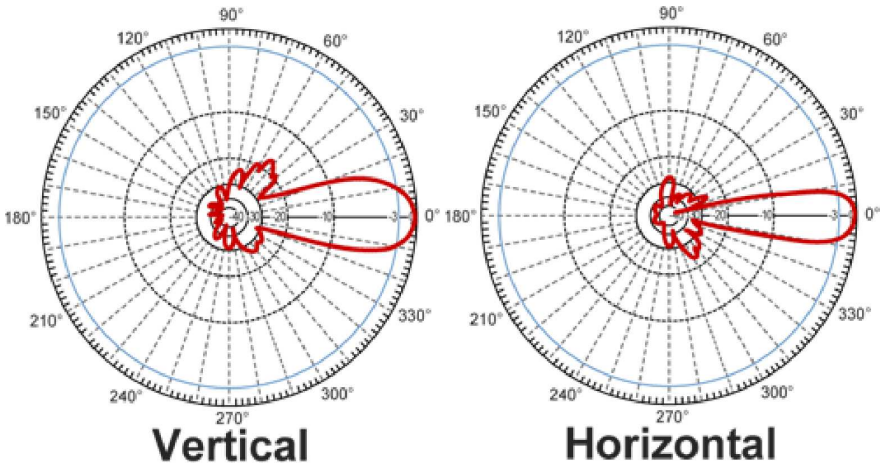

Figure 2.2: Horizontal and vertical radiation patterns for a (highly directional) 24 dBi parabolic dish antenna. Image taken from L-COM antenna specifications [125].

unmoving obstacles it is referred to as *shadowing*, *slow-fading*, or *large-scale fading*. When it is caused by small transient obstacles, and varies with time, it is called *scattering*, *fast fading*, or *small-scale fading*.

When the signals interact with the environment, they can be delayed by reflections, or frequency-shifted by diffractions. Mobile transceivers also incur frequency shift due to Doppler spreading. Frequency shifts and delay spread both contribute to small scale fading.

2.1.2 Path Loss

The *geometry* of the antennas that the transmitter and receiver use emphasizes signals arriving from some directions over others. An omnidirectional antenna emphasizes signals in the azimuthal plane and de-emphasizes signals arriving from above or below. As a result, the gain pattern tends to be shaped like a donut, as can been seen in figure 2.3. A directional antenna, such as a patch panel, parabolic dish, or sector, typically emphasizes signals arriving from a single direction (*lobe*) within some *beamwidth*. The gain pattern of these antennas more closely resembles a baseball bat, as can be seen in figure 2.2. However, perfect isolation is impossible and geometries that emphasize a single direction also have substantial gain in other directions (*side lobes* and *back lobes*) as a result. Antenna gain is typically measured in dBi, which is decibels relative to an isotropic transmitter (an isotropic transmitter's gain pattern is a sphere).

If the transmitter's radio has a transmit power of P_{tx} Watts (W) and an antenna gain of G_t dBi, then

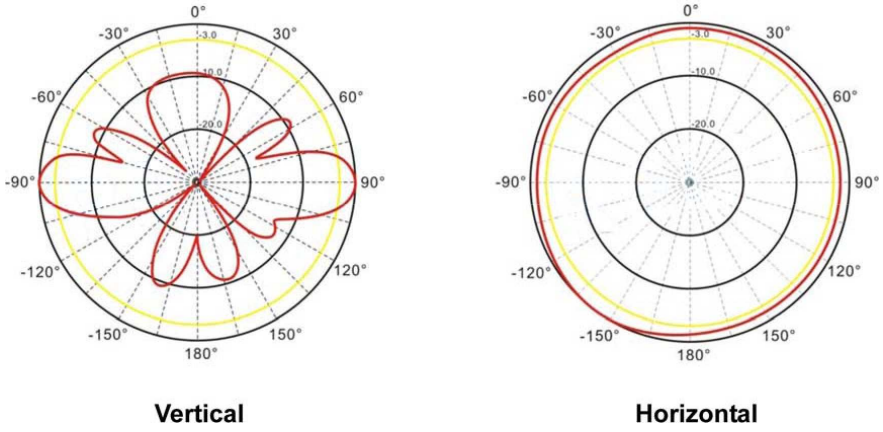

Figure 2.3: Horizontal and vertical radiation patterns for 7 dBi colinear omnidirectional antenna. Image taken from L-COM antenna specifications [125].

the total Effective Isotropic Radiated Power (EIRP) is $P_{tx} * G_{tx}$. In the log domain, P_{tx} is given in dBm, which is decibels relative to a mW, and the EIRP is simply $P_{tx} + G_{tx}$. The entire radio link can then be summarized by the common log-domain link budget equation:

$$P_{rx} = P_{tx} + G_{tx} + G_{rx} - PL \tag{2.1}$$

with P_{rx} and G_{rx} being the power received at the receiver and the receiver's antenna gain in the direction of the transmitter. Here, the PL term includes all attenuation due to path loss. This formula describes the aggregate gain and attenuation of many competing signals. It also assumes that our radio link is isolated from any sources of external noise in the environment (i.e., thermal noise and interference from other transmitters). Commonly, the signal quality at a given point is written as the ratio between Signal and Noise: $SNR = P_{rx} - N$ (in the log domain). Alternately, if interference from a known set of interferers is included, the Signal to Interference and Noise Ratio (SINR) is defined as:

$$SINR = P_{rx} - \left(N + \sum_{j}^{n} I_j \right) \tag{2.2}$$

For a given receiver design and modulation scheme, there is a known relationship between Signal to Noise Ratio (SNR) and bit error rate. Using this relationship, we can determine the minimum detectable signal for a given radio as a function of the acceptable error rate: $MDS(P_e)$, where P_e is the probability of bit error. Then, determining the points that are covered is simply the set of receiver locations that satisfy the inequality:

$$P_{tx} + G_{tx} + G_{rx} - PL \geq MDS(P_e) \tag{2.3}$$

Because the P and G terms are known for a given link, the difficulty becomes predicting the quantity PL given what we know about the environment and the radio link. In the case of measurement-based approaches, the complementary problem involves interpolating the PL value for the points we have not measured.

As it is defined here, a model's task is to predict the value of $L_t + L_s$ in this log-domain equation:

$$PL = L_t + L_s + L_f(t) \tag{2.4}$$

where L_t is the trivial free-space path loss, L_s is the loss due to shadowing (slow fading) from large unmoving obstacles like mountains and buildings, and $L_f(t)$ is the small-scale fast fading due to destructive interference from multipath effects and small scatterers (which varies with time t). Small-scale fading is often both time and frequency selective, meaning that it varies with time and frequency. Models cannot, without perfect knowledge of the environment, be expected to predict the quantity $L_f(t)$. In most applications, this additional error is computed "stochastically" using a probability distribution (often Raleigh, although Ricean and m-Nakagami are popular). In this way, frequency and time selective fades can be simulated, if not predicted exactly, which allows for the analysis of their effect on modulation schemes (e.g., [90, 213]). In the following sections, the many methods proposed for predicting the value of $L_t + L_s$ and the distribution of $L_f(t)$ are discussed.

2.2 Modeling Path Loss *A Priori*

The models discussed in this section are *a priori*, meaning they make predictions using only available prior knowledge and do not use explicit measurements in their predictions. Hence, these models are most appropriate for making predictions in situations where it is impossible or difficult to obtain measurements. We subdivide these models into six categories:

(1) Theoretical/Foundational Models (§2.2.1)

(2) Basic Models (§2.2.2)

(3) Terrain Models (§2.2.3)

(4) Supplementary Models (§2.2.4)

(5) Stochastic Fading Models (§2.2.5)

(6) Many-Ray (Ray-Tracing) Models (§2.2.6)

Name	Short Name	Category	Coverage Notes	Citations	Year
Friis' Free-space	friis	Foundational	$d > 2a^2/\lambda$	[77]	1946
Egli	egli	Basic	$30MHz < f < 3GHz$	[69, 206]	1957
Hata-Okumura	hata	Basic	$1km < d < 10km$; $150 <= f <= 1500MHz$ $30 <= h_1 <= 200m$; $1 <= h_1 <= 20$	[157]	1968
Edwards-Durkin	edwards	Basic/Terrain		[68, 62]	1969
Allsebrook-Parsons	allsebrook	Basic/Terrain	$f \in 85, 167, 441MHz$; Urban	[21, 62]	1977
Blomquist-Ladell	blomquist	Basic/Terrain		[37, 62]	1977
Longley-Rice Irregular Terrain Model (ITM)	itm	Terrain	$1km < d < 2000km$ $20MHz < f < 20GHz$	[98, 99]	1982
Walfisch-Bertoni	bertoni	Basic		[235]	1988
Flat-Edge	flatedge	Basic		[203]	1991
TM90	tm90	Basic	$d <= 10miles; h_1 <= 300feet$	[58]	1991
COST-231	cost231	Basic	$1km < d < 20km$;	[48]	1993
Walfisch-Ikegami	walfish	Basic	$200m < d < 5km$; $800MHz < f < 2GHz$; $4m < h_b < 50m$; $1m < h_m < 3m$	[48, 153, 34]	1993
Two-Ray (Ground Reflection)	two.ray	Foundational		[183, 206, 165]	1994
Hata-Davidson	davidson	Basic	$1km < d < 300km$; $150MHz < f < 1.5GHz$; $30m < h_b < 1500m$; $1m < h_m < 20m$	[38, 153]	1997
Oda	oda	Basic		[154]	1997
Erceg-Greenstein	erceg	Basic	$f \approx 1.9GHz$; Suburban	[71]	1998
Directional Gain Reduction Factor (GRF)	grf	Supplementary	Dir. Recv. Ant.,$f \approx 1.9GHz$	[85]	1999
Rural Hata	rural.hata	Basic	$f \in 160, 450, 900MHz$; Rural (Lithuania)	[143]	2000
ITU Terrain	itu	Terrain		[206, 107]	2001
Stanford University Interium (SUI)	sui	Basic	$2.5 < f < 2.7GHz$	[72, 19]	2001
Green-Obaidat	green	Basic		[84]	2002
ITU-R	itur	Basic	$1km < d < 10km$; $1.5GHz < f < 2GHz$; $30m < h_b < 200m$; $1m < h_m < 10m$	[107, 153]	2002
ECC-33	ecc33	Basic	$1km < d < 10km$; $700 <= f <= 3000MHz$ $20 <= h_1 <= 200m$; $5 <= h_1 <= 10$	[66, 19]	2003
Riback-Medbo	fc	Supplementary	$460MHz < f < 5.1GHz$	[190]	2006
ITU-R 452	itur452	Terrain		[109]	2007
IMT-2000	imt2000	Basic	Urban	[78]	2007
deSouza	desouza	Basic	$f \approx 2.4GHz; d < 120\,m$	[61]	2008
Effective Directivity Antenna Model (EDAM)	edam	Supplementary	Directional Antennas; $f \approx 2.4GHz$	[28]	2009
Herring Air-to-Ground	herring.atg	Basic	$f \approx 2.4GHz$	[94]	2010
Herring Ground-to-Ground	herring.gtg	Basic	$f \approx 2.4GHz$	[94]	2010

Table 2.1: *A priori* models studied along with their categorization, required input, coverage remarks, relevant citations, and year of (initial) publication.

Each category and its respective subcategories are discussed in turn in the following subsections. Table 2.1 provides a chronological list of the models discussed here and provides their major category, coverage, and initial publication.

2.2.1 Theoretical/Foundational Models

The first models worth considering are purely analytical models derived from the theory of idealized electromagnetic propagation. Although these models are questionably accurate, they are simple to understand and implement. As a result they have been widely adopted into network simulators and other applications, and often serve to compute a minimum loss for other, more complex, models.

2.2.1.1 Free-space Between Isotropic Antennas

In [77], Friis proposed a basic formula for free-space transmission loss:

$$\frac{P_{rx}}{P_{tx}} = \frac{A_{rx}A_{tx}}{d^2\lambda^2} \tag{2.5}$$

This formula describes the ratio between received power (P_{rx}) and transmitted power (P_{tx}) in terms of the effective area of the transmitting antenna (A_{tx}), receiving antenna (A_{rx}), the distance between (d) in meters, and the wavelength of the carrier (λ) in meters. For ideal isotropic antennas, this formula can be simplified to:

$$\frac{P_{rx}}{P_{tx}} = \left(\frac{\lambda}{4\pi d}\right)^2 \tag{2.6}$$

Or, more commonly, we solve for the power at the receiver in terms of the power from the transmitter and the path loss:

$$P_{rx} = P_{tx}\left(\frac{\lambda}{4\pi d}\right)^2 \tag{2.7}$$

Converting equation 2.7 to take distance in km instead of m, frequency in MHz instead of wavelength in m, and converting the linear domain power units (W) to log domain units (dBm), gives the commonly

d	distance between transmitter and receiver along line of sight path in km
d_m	distance between transmitter and receiver along line of sight path in m ($1000d$)
h_{tx}/h_{rx}	height of transmitter/receiver above ground in m
P_{tx}/P_{rx}	power produce by transmitter/received by receiver
f	carrier frequency in MHz
λ	carrier wavelength in m
g_{tx}/g_{rx}	gain of the transmitters/receiver's antenna in the azimuthal direction of the transmitter
θ	angle from transmitter to receiver in azimuthal plane relative to true north
θ'	angle from receiver to transmitter ...
ϕ	angle of elevation between transmitter and receiver relative to horizontal (inclination)
ϕ'	angle from receiver to transmitter ...
$U(a,b)$	a uniformly distributed random variable between a and b (inclusive)
$N(\mu,\sigma)$	a normally distributed random variable of mean μ and standard deviation σ
$LN(\mu,\sigma)$	a lognormally distributed random variable of mean μ and standard deviation σ
R	the radius of the earth in m ($\approx 6.371 * 10^6$)
C	the speed of light in m/s ($\approx 299.792 * 10^6$)
ϵ_r	relative permittivity (of obstructing material)

Table 2.2: Commonly used mathematical symbols.

seen reference equation for path loss as a function of carrier frequency and distance:

$$P_{rx} = P_{tx} - (20log_{10}(d) + 20log_{10}(f) + 32.45) \tag{2.8}$$

Where power in decibels relative to a milliwatt (dBm) can be obtained from power in Watts (W) using this conversion:

$$P_{dBm} = 10log_{10}(P_{mW}) \tag{2.9}$$

2.2.1.2 Flexible Path Loss Exponent

Whereas Friis' equation assumes that signal degrades as a function of d^2, a common extension to No(n) Line of Sight (NLOS) environments is to use a larger exponent. To allow for this, we simply substitute in α, which can be set to any value greater than zero, but is most commonly set to 2:

$$P_{rx} = P_{tx} - (10\alpha log_{10}(d) + 20log_{10}(f) + 32.45) \tag{2.10}$$

Often, this model will be given relative to some reference distance d_0 (commonly 100m), where the assumption is that several measurements are made at this distance, and those values are used to fit a slope:

$$P_{rx} = P_{tx} - (10\alpha log_{10}(d/d_0) + 20log_{10}(f) + 32.45) \tag{2.11}$$

2.2.1.3 Ground Reflection

As a modest extension to the free-space path loss model, the Two-Ray Ground Reflection model considers a second path that reflects from the ground between the transmitter and receiver [183, 206, 165]. First, we calculate the break distance:

$$d_c = (4\pi h_{tx} h_{rx})/\lambda \tag{2.12}$$

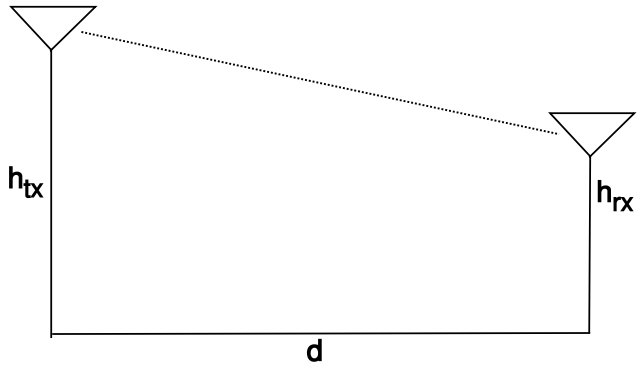

Figure 2.4: Schematic of link geometry used by basic models.

where h_{tx} and h_{rx} are the heights of the transmitter and receiver antennas, respectively (in m). For distances shorter than this break distance, we simply use Friis' equation as the receiver is not far enough away to receive a substantial ground reflected path loss. For distances longer than the break distance, we use the modified path loss formula:

$$P_r = \frac{P_{tx} h_{tx}^2 h_{rx}^2}{d^4} \tag{2.13}$$

In [154], Oda *et al.* propose a minor extension to this model where the plane of reflection is considered to be above the nominal ground clutter, and a factor for probability of collision per unit distance is considered. By adjusting this height offset (h_0), the reflectivity coefficient (R) and this negative exponentially weighted factor, one can coax the simple Two-Ray model into more closely fitting some types of measured data.

2.2.2 Basic Models

Basic models are the most numerous of the model types. They compute path loss along a single path and often use corrections based on measurements made in one or more environments. In general, they use the distance, carrier frequency, and transmitter and receiver heights as input. Figure 2.4 gives a schematic of the basic link geometry. Some models also have their own esoteric parameters to select between different modes of computation or fine tuning. Here we subdivide these models into deterministic and stochastic. The stochastic models use one or more random variables to account for channel variation (and hence, can predict

a distribution instead of a median value).

2.2.2.1 Egli

The Egli Model [69] is an early empirical model based on measurements made in New York City and parts of New Jersey by John Egli. The simplified version, based on extracting a model from numerous graphs and nomograms [62] and [34] is:

$$P_{rx} = P_{tx} - 20log_{10}(f) + 40log_{10}(d) - 20log_{10}(h_{tx}) + k \tag{2.14}$$

with

$$k = \begin{cases} 76.3 - 10log_{10}(h_{rx}) & h_{rx} \leq 10 \\ 85.9 - 20log_{10}(h_{rx}) & h_{rx} > 10 \end{cases} \tag{2.15}$$

2.2.2.2 Green-Obaidat

The Green-Obaidat model suggested in [84] is a small modification to free-space path loss that adjusts for the relative heights of the transmitter and receiver and uses a path loss exponent of $\alpha = 4$:

$$P_{rx} = P_{tx} - (40log_{10}(d) + 20log_{10}(f) - 20log_{10}(h_{tx}h_{rx})) \tag{2.16}$$

In this model, d is given in km, h_{tx} and h_{rx} in m, and f in MHz. The authors perform minimal validation using 802.11 devices operating at 2.4 GHz. This model is one of several that extends basic models to include the relative height of nodes in their calculations—in this case, the heights are multiplied.

2.2.2.3 Edwards-Durkin

The Edwards-Durkin model [68] simply sums classical free-space loss (lf) with an additional correction due to plane earth propagation loss from Bullington [42]:

$$lp = 118.7 - 20log10(h_{rx}) - \tag{2.17}$$

$$20log10(h_{tx}) + 40log10(d)$$

$$PL = lf + lp \tag{2.18}$$

The constants in this formula are fitted from empirical measurements made in the United Kingdom by Durkin [67]. In [62], Delisle updates this model with a statistical terrain diffraction loss estimate ($ld(\Delta h)$, described in section 2.2.4.2) and leaving out the free-space term:

$$PL' = lp + ld(\Delta h) \tag{2.19}$$

2.2.2.4 Blomquist-Ladell

The Blomquist-Ladell model [37] is similar in construction to the Edwards-Durkin model. It computes an excess plane earth loss, with a correction factor, and sums it with classical free-space loss. As with the Edwards-Durkin model, it can be extended with a statistical terrain diffraction loss estimate. The fitted constants in this model were derived from measurements in the VHF and UHF bands over rolling terrian in Sweden.

The excess plane earth loss is computed as:

$$fb = 10.0log10\,|a_{tx}a_{rx}| + y \tag{2.20}$$

$$a_i = \frac{4\pi h_i^2}{\lambda d_m} + \frac{\lambda \epsilon_r^2}{\pi d(\epsilon_r - 1)} \tag{2.21}$$

With d being the link distance in meters, and the correction factor, y:

$$y = \begin{cases} -2.8x & x < 0.53 \\ 6.7 + 10log10(x) - 10.2x & \text{o.w.} \end{cases} \tag{2.22}$$

$$x = (2\pi/\lambda)^{1/3}(kR)^{-2/3}d \tag{2.23}$$

Finally, the path loss is summed with free-space loss:

$$s_+ = lf + \sqrt{fb^2 + ld(\Delta h)^2} \tag{2.24}$$

$$s_- = lf - \sqrt{fb^2 - ld(\Delta h)^2} \tag{2.25}$$

$$PL = \begin{cases} s_+ & fb \leq 0 \\ s_+ & fb > 0, \leq |ld(\Delta h)| \\ s_- & fb > 0, > |ld(\Delta h)| \end{cases} \tag{2.26}$$

$$\tag{2.27}$$

Where $ld(\Delta h)$ is the statistical terrain diffraction loss estimate described below in section 2.2.4.2, lf is the basic free-space loss calculated as in equation 2.8, k is the earth radius factor (typically 4/3), and ϵ_r is the dielectric constant (relative permittivity) of the ground (Delisle recommends 10 for dry earth).

2.2.2.5 Allsebrook-Parsons

The Allsebrook-Parsons model [21] is an extension to the Blomquist-Laddell model that adds an additional loss due to buildings. The authors based the empirical adjustment on measurements taken in British cities. The model also suggests a constant additional loss (named γ here) of 13 dB for frequencies above 200 MHz[1] .

$$lb = 20log10\left(\frac{h_0 - h_{rx}}{548\sqrt{d_2 10^{-3} f}}\right) + 16 \tag{2.28}$$

$$PL = PL_b + lb + \gamma \tag{2.29}$$

where PL_b is the path loss computed by the Blomquist-Ladell model, h_0 is the average height of buildings in the neighborhood of the mobile station in m, and d_2 is the average street width in m.

[1] The validity of this correction is questioned in [62].

2.2.2.6 deSouza-Lins

In [61], de Souza and Lins present an entirely empirical model explicitly fitted to data collected at 2.4 GHz. This model is a function of distance (in meters) and relative humidity percentage (h):

$$P_{rx} = P_{tx} - (\beta_0 + \beta_1 log_{10}(d) + \beta_2 d + \beta_3 log_{10}(h)) \tag{2.30}$$

Although the authors claim very impressive performance at the sites (two indoor, two outdoor) they study (from which the fitted β parameters are derived), the short distances studied ($< 120\,m$) suggest that this model may be inappropriate for modeling lengthier links.

2.2.2.7 TM90

In [58], the authors propose a propagation model intended for suburban areas and for propagation distances less than 10 miles. This model is very simple, using a flexible path loss exponent model with $\alpha = 4$, accounting for antenna heights as in the Hata-Okumura model, and adding an additional loss for average building penetration (outdoor-indoor interface loss). This model is the FCC recommended model for shorter propagation distances (as opposed to the Irregular Terrain Model (ITM), which is recommended by the FCC for long links).

2.2.2.8 Hata-Okumura

The Hata-Okumura model is an empirical model where measurements made by Okumura in and around Tokyo, Japan are approximated with equations proposed by Hata [34, 157]. The model is considered valid for frequencies from 150 MHz to 1500 MHz, transmitter heights between 30 m and 200 m, receiver heights between 1 m and 10 m, and distances greater than 1 km. The model takes an additional environment parameter that can be one of “open”, “suburban”, “urban medium”, or “urban large”, which selects among different modes of computation for differing levels of environment complexity (as related to population density).

The correction factors are first computed, based on the enviromnental complexity:

$$a = \begin{cases} 3.2log10((11.75h_{rx})^2) - 4.97 & \text{large city} \\ h_{rx}(1.1log10(f) - 0.7) - (1.56log10(f) - 0.8) & \text{o.w.} \end{cases} \tag{2.31}$$

$$k = \begin{cases} 2log10(f/28)^2 + 5.4 & \text{suburban} \\ 4.78log10(f)^2 - 18.33 & \text{open} \\ log10(f) + 40.94 & \\ 0 & \text{o.w.} \end{cases} \tag{2.32}$$

(2.33)

Then, the final path loss is computed by offsetting a constant (transmitter height adjusted) free-space path loss (b):

$$b = 69.55 + 26.16log10(f) - 13.82log10(h_{tx}) \tag{2.34}$$

$$PL = b - a + log10(d) * (44.9 - 6.55log10(h_{tx})) - k \tag{2.35}$$

Due to the popularity of the Hata-Okumura model, there have been numerous extensions and corrections:

COST-Hata/Extended Hata

The COST-Hata model is an extension of the Hata-Okumura model to cover frequencies up to 2000 MHz. It was proposed as part of the COST-231 [34, 78, 48].

First the correction factors a and c are computed:

$$a = h_{rx}(1.1log10(f) - 0.7) - \tag{2.36}$$
$$(1.56log10(f) - 0.8)$$

$$c = \begin{cases} 3.0 & \text{large city} \\ 0.0 & \text{o.w.} \end{cases} \tag{2.37}$$

$$\tag{2.38}$$

Then, as before the path loss is computed by offsetting a free-space path loss computation (b):

$$b = 46.33 + 33.9log10(f) - \tag{2.39}$$
$$13.82log10(h_{rx})$$

$$PL = b - a + (44.9 - 6.55log10(h_{rx})) * \tag{2.40}$$
$$log10(d) + c$$

Hata-Davidson

In the Telecommunications Industry Association (TIA) recommendation TSB-88-B, an extension to the Hata-Okumura model is proposed, which provides corrections for long links (up to 300 km) and high transmitters (up to 2500 m) [223, 153]:

$$a = \begin{cases} 0.62137(d - 20.0)* & d \geq 20km \\ (0.5 + 0.15log10(\frac{h_{tx}}{121.92})) & \\ 0 & \text{o.w.} \end{cases} \tag{2.41}$$

$$s_1 = \begin{cases} 0.174(d - 64.38) & d \geq 64.38km \\ 0 & \text{o.w.} \end{cases} \tag{2.42}$$

$$s_2 = \begin{cases} |0.00784log10(9.98/d)| & h_{tx} > 300m \\ (h_{tx} - 300.0) & \\ 0 & \text{o.w.} \end{cases} \tag{2.43}$$

$$s_3 = (f/250)log10(1500/f) \tag{2.44}$$

$$s_4 = \begin{cases} 0.112log10(1500/f)(d - 64.38) & d > 64.38 \\ 0 & \text{o.w.} \end{cases} \tag{2.45}$$

$$PL_{davidson} = PL_{hata} + (a - s1 - s2 - s3 - s4) \tag{2.46}$$

Where a, s_1, s_2, s_3, and s_4 are used to correct the calculation in equation 2.36.

ECC-33

In [66], the Electronic Communication Committee (ECC) within the European Conference of Postal and Telecommunications Administrations (CEPT) extend the coverage up to 3,500 MHz:

$$afs = 92.4 + 20.0log10(d) + 20.0log10(f) \tag{2.47}$$

$$abm = 20.41 + 9.83log10(d) + 7.894log10(f) + 9.56log10(f)^2 \tag{2.48}$$

$$gb = log10(hb/200)(13.958 + 5.8log10(d)^2) \tag{2.49}$$

$$gr = \begin{cases} (42.57 + 13.7 * log10(f))(log10(h_{rx}) - 0.585) & \text{medium city} \\ 0.0 & \text{o.w.} \end{cases} \tag{2.50}$$

$$PL_{ecc33} = afs + abm - gb - gr \tag{2.51}$$

ITU-R/CCIR

The International Radio Consultive Committee (CCIR) (now the International Telecommunications Union Radiocommunication Sector (ITU-R)) proposed a version of the Hata-Okumura model, which takes a real-valued parameter, the percentage of area covered by buildings (bp), instead of a discrete environment class. This model is an attempt at correcting systematic underestimations observed in the Hata-Okumura model and is in essence the Hata-Okumura model for "urban-medium" environments with an additional correction factor related to the new parameter [153]:

$$a = (1.1log10(f) - 0.7)h_{rx} - (1.56log10(f) - 0.8) \tag{2.52}$$

$$b = \begin{cases} 30 - 25log10(bp) & bp > 0 \\ 0 & \text{o.w} \end{cases} \tag{2.53}$$

$$c = 69.55 + 26.16log10(f) - 13.82log10(h_{tx}) \tag{2.54}$$

$$PL_{ccir} = c - a + (44.9 - 6.55log10(h_{tx}))log10(d) - b \tag{2.55}$$

Rural Hata

In [143], Medeisis *et al.* propose a correction for the classic Hata-Okumura model as defined in ITU-R 529 to correct for systematic overestimations of path loss in rural terrain. Their model proposes new fitted values for the path loss exponent and fixed offset to replace those that are defined in the default model. These fits are obtained from data collected using a simple random sampling scheme in rural Lithuania at three frequencies below 900 MHz. In addition to this, the authors propose a method to do site-specific fitting in a similar way so that their approach can be used in other environments and at other frequencies.

The loss in dBuV/m (decibels relative to a microVolt per meter) is given by the equation:

$$e_{sys} = -6.16log(f) + 13.82 * log(h_{tx}) + ((1.1log(f) - 0.7)h_{rx} - (1.56log(f) - 0.8)) \tag{2.56}$$

$$\gamma_{sys} = \gamma(44.9 - 6.55log(h_{tx})) \tag{2.57}$$

$$PL'_{rural} = e_0 + e_{sys} + \gamma_{sys}log(d) \tag{2.58}$$

To convert this value to dBm so it is consistent with our other equations, we use the following conversion [18]:

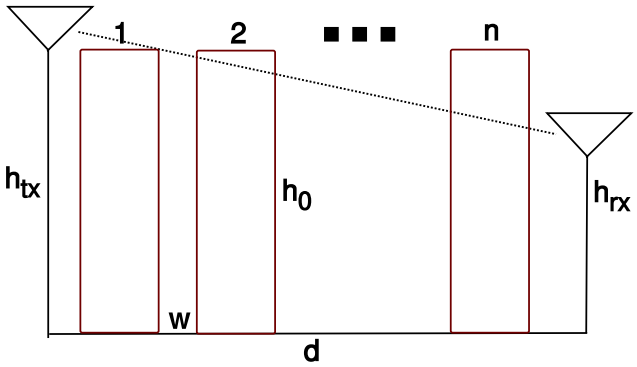

Figure 2.5: Schematic of link geometry used by the Flat-Edge family of basic models.

$$PL_{rural} = -(PL'_{rural} + g_{rx} - 20log(f) - 77) \tag{2.59}$$

2.2.2.9 Flat-Edge

The Flat-Edge model, proposed by Saunders and Bonar [203] takes a very different approach as compared to the Hata family of models. Saunders and Bonar propose a model that computes approximate knife-edge diffraction losses due to multiple obstructions (buildings) that are regularly spaced. Figure 2.5 provides a schematic of this setup. The model takes as parameters the number of obstructions between the transmitter and receiver (n), the constant distance between them (w), and their constant height (h_0). The assumption is that there is a transmitter either above or below a series of obstacles of the constant size and spacing and the receiver is below the top of the buildings. The model works by summing the loss due to Fresnel obstruction by the obstacles, the basic free-space propagation loss (lf), computed using equation 2.8, and the loss due to diffraction over the final obstruction.

First, the value of t is calculated:

$$t = \phi\sqrt{\frac{\pi w}{\lambda}} \tag{2.60}$$

If $1 \leq n \leq 100$ and $-1 \leq t < 0$, then the approximate fit due to Barclay [34] is used:

$$ln = -(3.29 + 9.90log10(t) - (0.77 + 0.26log10(n))) \tag{2.61}$$

If, however, this is not the case, then a complicated series of Fresnel calculations are required to compute ln. Those equations are well summarized in [203] Appendix B.3. The additional loss due to diffraction over the final obstruction is calculated using the method of Ikegami [100].

$$le = \begin{cases} 10log10(f) + 10log10(sin(\phi)) + 20log10(h_0 - h_{rx}) - \\ 10log10(w) - 10log10(1 + 3/lr^2) - 5.8 & h_{rx} < h_0, \phi \neq 0 \\ 0 & \text{o.w.} \end{cases} \tag{2.62}$$

where lr is the refraction loss fraction, commonly set to 0.25. Finally, the sum is computed:

$$PL_{flatedge} = ln + lf + le \tag{2.63}$$

2.2.2.10 Walfisch-Bertoni

The Walfisch-Bertoni model is the limiting case of the Flat-Edge model when the number of buildings is large enough for the field to settle [34]. Hence, this model takes as parameters the distance between obstructions and their nominal size, but not the number of them, which is implicit to the calculation.

$$la = \begin{cases} log10((w/2) + (h_0 - h_{rx})^2) - 9log10(w) + \\ 20log10(atan((2.0(h_0 - h_{rx}))/w)) & h_{rx} \leq h_0 \\ 0 & \text{o.w} \end{cases} \tag{2.64}$$

$$c = \begin{cases} 18log10(h_{tx} - h_0) & h_{tx} - h_0 > 0 \\ 0 & \text{o.w} \end{cases} \tag{2.65}$$

$$lex = 57.1 + log10(f) + 18log10(d) - c - 18log10(1 - d^2/(17(h_{rx} - h_0))) \tag{2.66}$$

$$PL_{bertoni} = lf + lex + la \tag{2.67}$$

where lf is the trivial free-space loss computed with equation 2.8.

2.2.2.11 Walfisch-Ikegami

The European Cooperation in the field of Scientific and Technical Research Action 231 (COST-231)/Walfisch-Ikegami is a compromise proposal by the COST-231 that combines the Walfisch-Bertoni model with an additional reflection down to the receiver using the Ikegami model [100] along with some empirical corrections from measurements [34]. The model distinguishes between Line of Sight (LOS) propagation and NLOS and uses different calculations for each. In addition to the expected parameters describing the geometry of the LOS path, this model requires specification of the constant building height, street width (w), distance between buildings (b, such that $b - w$ is the nominal building width), the angle of the incident wave to the street (π radians for vertically polarized antennas, 0 for horizontal), and the building size (either "medium" or "large").

For NLOS links, the model includes calculations for excess loss above free-space loss due to roof-to-street diffraction loss and multiscreen diffraction loss. After calculating this excess loss, if it is positive, it is summed with the free-space loss and used. Otherwise, uncorrected free-space loss is returned. For LOS links, the returned value is free-space loss with a fudge factor to attempt to avoid underestimates: $6 * log_{10}(50 * d)$. Because this model is reasonably complicated, we refer the interested reader to the excellent slides maintained by the National Institute of Standards and Technology (NIST) [153] for further details.

The remaining basic models include a random variate (stochastic) term that attempts to capture the time-varying nature of the wireless channel due to small scale fading.

2.2.2.12 Herring

The Herring model is a recent proposal by Herring *et al.* [94]. The model proposes two distinct models, one for Air-to-Ground (ATG) communications and one for Ground-to-Ground (GTG), both of which are based on fits to data collected by the authors at 2.4 GHz in Cambridge, Massachusetts. The ATG model is a simple error term on top of the free-space path loss model:

$$P_{rx} = P_{tx} - (lf + N(30, 8.3)) \tag{2.68}$$

where lf is calculated as in equation 2.8 and $N(30, 8.3)$ is a random Gaussian with mean 30 and standard deviation of 8.3. The GTG model is slightly more complex. It first computes a random Gaussian path loss exponent with uniform random offset:

$$\alpha = U(2, 5) + N(0, 0.22) \tag{2.69}$$

This path loss exponent is then used along with a larger excess loss value:

$$P_{rx} = P_{tx} - (lf(\alpha) + N(40, 5.5)) \tag{2.70}$$

where $lf(\alpha)$ is computed as in equation 2.10.

2.2.2.13 Erceg-Greenstein

In [71], Erceg *et al.* present a measurement-based model for path loss around 1.9 GHz using a large data set collected by AT&T in suburban locations around New Jersey. It is a fitted model that combines a fit for median path loss at some distance d and a randomly distributed variation:

$$\begin{aligned} PL = A + 10(a - b * h_{tx} + \\ (\frac{c}{h_{rx}})log10(\frac{d}{d_0}) + x10log10(\frac{d}{d_0}) + \\ y\mu_\sigma + yz\sigma_\sigma \end{aligned} \tag{2.71}$$

where the values of $a, b, c, \sigma_\gamma, \mu_\sigma$, and σ_σ are fitted parameters for each of the three terrain categories: hilly with moderate to heavy tree density (A), hilly with light tree density or flat with moderate to heavy tree density (B), or flat with light tree density (C). The value A is the trivial free-space path loss (from equation 2.8, for instance) at some reference distance (d_0, usually 100 m). And, x, y, and z are normally distributed random variables between -2 and 2 (x is between -1.5 and 1.5).

2.2.2.14 IMT-2000: Pedestrian Environment

Three path loss models for IMT-2000/3G are provided in [78], one for the indoor office environment, one for the outdoor to indoor and pedestrian environment, and one for the vehicular environment. It is the pedestrian model which we describe here, which is simply equation 2.10 with $\alpha = 4$, a constant (optional) offset for building penetration loss (k_1) and a lognormally distributed offset to account for shadowing loss (k_2):

$$P_{rx} = P_{tx} - (40log_{10}(d) + 30log_{10}(f) + k_1 + k_2 + 21) \tag{2.72}$$

with

$$k_1 = \begin{cases} 18 & indoors \\ 0 & o.w. \end{cases} \tag{2.73}$$

and

$$k_2 = LN(0, 10) = e^{0+10N(0,1)} \tag{2.74}$$

where $LN(0, 10)$ is a lognormally distributed random variable with zero mean and a standard deviation of 10.

2.2.3 Terrain Models

Terrain models are similar to the basic models, but also attempt to compute diffraction losses along the line-of-sight path due to obstructions (terrain or buildings, for instance, see figure 2.6 for a schematic). They are an order of magnitude more complex, but are immensely popular especially for long propagation distances at high power in the VHF band (i.e., television transmitters). Because of the relative complexity of these models, the reader will need to refer to the citations for details of the implementations. Here, their functionality is summarized at a high level.

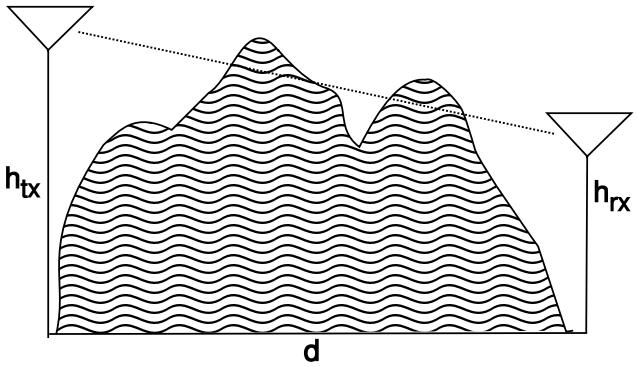

Figure 2.6: Schematic of link geometry used by terrain models.

2.2.3.1 ITU Terrain

The ITU terrain model is a simple model that combines free-space path loss with a single diffraction due to terrain [206, 107]. A Digital Elevation Model (DEM) is used to compute the loss due to the most significant path obstruction in terms of Fresnel zone blockage. In the event that the transmission path has no blockage, then free-space path loss (with an exponent of 2) is used. The radius of the first Fresnel zone is computed at the site of blockage:

$$f_1 = 17.3\sqrt{\frac{d_1 d_2}{fd}} \tag{2.75}$$

where d_1 is the distance from the transmitter to the obstruction, d_2 is the distance from the receiver to the obstruction, d is the total distance, and f is the carrier frequency. The constant, 17.3, is derived from equations governing the physical optics of Fresnel lenses. Then the additional path loss (outside of free-space) is used for this blockage:

$$al = -20.0h/f_1 + 10.0 \tag{2.76}$$

The model suggests that a negative loss due to the blockage (which is actually a gain, i.e., negative loss) or any loss less than 6 dB should be discarded. The maximum additional loss is then used to “correct” the free-space loss assumption.

2.2.3.2 ITU-R 452

The clear-air interference prediction algorithm described in ITU-R 452 [109] serves a fine example of the state of the art in terrain path loss models. This model makes a prediction of median path loss based on the sum of free-space path loss with several corrections:

(1) losses from knife-edge diffractions over terrain obstacles

(2) losses from absorption due to atmospheric gases (water vapor)

(3) losses from tropospheric scatter, ducting, coupling, and layer reflection in the atmosphere

(4) losses due to obstruction from the curvature of the earth

(5) additional clutter losses derived from land cover classification [106] near the transmitter and receiver

The model computes the path loss in terms of a confidence value p, which is the not-to-exceed probability. Using $p = 50$ computes a median value, $p = 100$ computes a worst-case value and $p = 0$ computes a best-case value.

In addition to p, the model takes a handful of other parameters: Δn, which is the radio refractivity of the earth between the transmitter and receiver (values between 35 and 60 are typical for the environments studied in this thesis), n_0, which is the surface level refractivity, and ω, which is the fraction of the path over water (i.e., for intercontinental links. $\omega = 0$ for all of our environments). This model is leaps and bounds more complex than those presented above, requiring a tremendous number of calculations often based on numerical approximations (i.e., knife-edge diffraction).

ITU-R 452 suggests additional extensions for modeling the interference due to hydrometers such as rain and weather cells. This adds substantial complexity to the algorithm with negligible benefit for many communications applications operating in the upper end of the VHF band. Indeed, many of the parameters computed by the ITU-452 model are negligible for commonly used communications frequencies (for instance, absorption due to atmospheric gases). In [237], Whitteker suggests a similar model which shares many of the attributes of ITU-R 452, with slightly less complexity.

2.2.3.3 Longley-Rice Irregular Terrain Model

The ITM [98, 99] may be the most widely known general purpose path loss model and is used in a number of popular network planning tools (e.g., [136, 54]). This model was developed by the NTIA in order to plan deployments of Very High Frequency (VHF) transmitters (i.e., broadcast television in the US). Hence, much like the ITU-R model, it is designed for very long transmission at high power from well-positioned transmitters. For this reason its applicability to modeling propagation in, e.g., urban microcells, is questionable at best. Much like ITU-R 452, the ITM computes excess loss from free-space by considering knife-edge diffractions at terrain obstacles, losses due to the curvature of the earth, and tropospheric scatter. The principle difference is that ITU-R 452 includes some calculation for local clutter losses based on land cover classification data, otherwise the models can be thought to be quite similar.

2.2.4 Supplementary Models

The next category of models are supplementary models, which cannot stand on their own, but are instead used to make corrections to existing (complete) models. Here we subdivide the models by the phenomenon they wish to correct for.

2.2.4.1 Frequency Coverage

The Riback-Medbo model [190] attempts to correct for the (ill) effects of using a model intended for one frequency at a different frequency. The algorithm the authors propose provides a fitted correction when given the computed path loss, the assumed frequency, the target frequency based on measurements they make a three different frequencies:

$$a = 0.09 \tag{2.77}$$

$$b = 256 * 10^6 \tag{2.78}$$

$$c = 1.8 \tag{2.79}$$

$$k = a(atan(f_0/b - c) - atan(f_0/b - c)) \tag{2.80}$$

$$PL_{fc} = PL_0 + 20log10(f/f_0) - k(PL_0 - A) \tag{2.81}$$

where k is the correction factor which is used to correct the path loss value (PL_0) at a given frequency (f_0) so that it is better able to predict the loss at the desired frequency (f). The value A is the trivial free-space loss (from equation 2.8) at the original frequency (f_0). The authors validate this model using a significant amount of data in a limited number of (suburban) environments, from which the empirical constants are derived.

2.2.4.2 Obstructions

Obstruction models account for losses due to specific obstructions along the main (or some secondary) path. They are the most numerous and varying of the supplementary models:

Atmospheric Gases

The effects due to absorption by atmospheric gases are minimal at UHF frequencies and totally negligible at higher frequencies. However, it is worth noting that such corrective models are available for water vapor and to a lesser extent for other gases (e.g., [110]).

Statistical Terrain Diffraction Estimate

Because terrain information is not always available and computing individual diffractions over terrain can be computationally costly, [62] proposes a method for computing an estimate of additional losses due to terrain. In addition to the geometry of the line-of-sight path, this approach makes use of a single parameter, Δh, which describes the "roughness" of the terrain. A value of ≈ 15 is considered minimal, ≈ 200 is used for hilly terrain, and ≈ 400 for very rugged terrain. In [62], Delisle *et al.* propose the use of this estimate in combination with other models, such as Allsebrook-Parsons, Blomquist-Ladell, and Edwards-Durkin. In

this way, it can be used to retrofit any basic model with corrections for losses from terrain obstacles and clutter.

Building-Transmission

The Building-Transmission model proposed by de Jong *et al.* in [59] attempts to model the loss due to transmission *through* a building in an urban environment. The authors attempt to isolate this effect from fades along other paths and instead present a statistical model for just the loss encountered by transmission through a number of representative buildings at 1.9 GHz. They find that on average there is a loss of approximately 2.1 dB/m at this frequency and use this to develop an algorithm to compute total transmission loss, including refraction at the exterior walls. For this model to be of use in practice, one must know the positions and shape of buildings along with the permittivity and conductivity of the buildings' outer surfaces.

Durgin-Rapaport

In [64], Durgin *et al.* make numerous measurements around residential homes and trees at 5.85 GHz. They use the collected data to come up with constant fitted values for losses associated with outdoor-indoor interface loss, loss due to single trees and stands of trees, as well as interior walls. These values are then used to form the basis of a "partition" path loss model that computes the final signal strength by computing the free-space loss and then combining it with the summed loss associated with each obstruction. A model of the same flavor and by the same authors is also proposed in [135], but for 2.4 GHz.

Vegetation

There have been a number of works that attempt to, in one way or another, model the losses due to vegetation obstructions. [108] proposes a very complex formulation that attempts to model the diffraction above and around a stand of trees. Parameters are provided for several species of trees, both in leaf and out of leaf. In [224], Torico *et al.* present an interesting but largely impractical theoretical model for loss due to trees. In this work, trees are modeled as a screen containing randomly placed cylindrical defractors. Although not useful for general prediction, this model demonstrates that vegetation can cause substantial losses. In [45], Chee *et al.* present a similar analytical model. The lack of availability of vector data describing the location, shape, and type of vegetation prohibits use in most applications. A more practical proposal is described in [134], where rain forest vegetation is modeled using four layers (ground, trees,

foilage, sky) with different propagation characteristics and interlayer ducting.

2.2.4.3 Directivity

Directivity models attempt to account for multipath (scattering) losses that are unique to situations where the transmitter, or more importantly the receiver, is using a directional antenna. The problem here is that directional antennas "emphasize" some azimuthal directions more than others, which leads to nontrivial multipath effects at the receiver. If the goal is to model a link involving directional antennas and the antenna is assumed isotropic (perhaps with the gain assumed to be equal to the maximum gain of the main lobe), a substantial deviation from reality can occur.

Gain Reduction Factor

In [85], Greenstein and Erceg find that there can be substantial gain reduction at the receiver. The authors make measurements in suburban New Jersey at 1.9 Ghz and fit a model to the effects. The model is fitted to the beamwidth of the receiving antenna and whether or not the measurements are made in winter (i.e., with or without leaves on trees).

$$i = \begin{cases} 1 & winter \\ -1 & o.w. \end{cases} \tag{2.82}$$

$$\mu = -(0.53 + 0.1i)log(\beta/360) + (0.50 + 0.04i)log(\beta/360)^2 \tag{2.83}$$

$$\sigma = -(0.93 + 0.02i)log(\beta/360) \tag{2.84}$$

$$PL_{grf} = N(\mu, \sigma) \tag{2.85}$$

where PL_{grf} is the additional gain or attenuation in dB and β is the beamwidth of the receiving antenna in degrees.

EDAM

The EDAM is a bin-fitted model derived from a large number of measurements made in several representative environments (multiple indoor and multiple outdoor environments) both with commodity hardware and with special purpose hardware. The result is a model that, when given an environment class,

will provide a correction as a function of the gain pattern at the receiver in the direction of the transmitter and vice versa. The model is also able to be used in a stochastic fashion for a repeated measures approach and with or without a Gaussian-distributed fading correction. The model is described in detail in appendix A and in [28, 30], it was shown that this model is better suited to making path loss predictions in simulation-based evaluations involving directionality than standard models.

2.2.5 Stochastic Fading Models

Stochastic fading models add a random variable to a path loss model to account for additional fading in the wireless channel. This includes fades due to scattering and multipath effects that are uncorrelated in measurements over small distances (i.e., less than a wavelength). These fades are selective in both time and frequency, meaning that attentuation may vary as a function of either (or both). Stochastic fading models are especially useful in the design of physical layer/data-link layer of wireless networks.

A number of measurement studies, find that residual error in an explicit fit to measurements follows a lognormal distribution. This is equivalent to adding a zero mean normally distributed error term X_σ to equation 2.10:

$$P_{rx} = P_{tx} - (10\alpha log_{10}(d) + 20log_{10}(f) + 32.45 + X_\sigma) \tag{2.86}$$

This model is commonly referred to as the "lognormal shadowing" model and can be used as an empirically corrected model where values of α and σ are determined from measurements. This is the most coarse stochastic fading model and is usually considered to be appropriate only for modeling large scale effects [183].

Small scale (time varying) stochastic fading models typically look to either Rayleigh, Ricean, or Nakagami distributions. The inquisitive reader can refer to the excellent treatment by Skylar of Rayleigh and Ricean fading in [210] or [246, 148] for discussions of the Nakagami distribution. Some low-level applications may choose to explicitly model inter-symbol interference by determining the delay spread of arriving signals, as observed at the reciever, from a representative distribution. In [86], for instance, Greenstein et

al., show that both delay-spread and path gain appear to be lognormally distributed in their measurements at 900 MHz.

Barclay-Okumura

The Barclay-Okumura model is a simple model for stochastic fading proposed by Barclay in [34] based on data collected by Okumura. It can operate in either "urban" or "suburban" mode, and computes a zero-mean Gaussian distributed fade with standard deviation σ:

$$a = \begin{cases} 5.2 & urban \\ 6.6 & suburban \end{cases} \tag{2.87}$$

$$\sigma = 0.65 log_{10}(f)^2 - 1.3 log_{10}(f) + a \tag{2.88}$$

2.2.6 Many-Ray Models

Many-ray models are typically referred to as ray-tracing or ray-launching models in the literature. In the taxonomy proposed here, they are called "many-ray" models to highlight the way in which they differ from all of the aforementioned models: they attempt to calculate the path loss by summing the loss along many distinct paths instead of only the line-of-sight (LOS) path. These models require substantial and precise knowledge about the environment. Two-and-three dimensional vector models of buildings and interfering structures are the most commonly used data. These models trace the interaction of many individual paths and these obstacles, computing reflection, refraction, and diffraction using the UTD, or an equivalent numerical approximation. As a result, they are able to compute not only the median path loss predicted at the receiver, but also the delay spread (which can be used to compute Inter-symbol Interference (ISI)) and frequency shift (which can be used to model frequency-selective fading effects) of arriving signals.

Early papers in this area include the work of Ikegami *et al.* in [100] and Vogler in [231], where it is proposed that mean field strength be calculated by computing diffractions and reflections from building vector data. Some work has been done to increase the accuracy and speed of calculating diffractions (e.g., [203, 242] and the comparative discussion in [65]).

The early applications of these ideas were applied in two-dimensional ray-tracing models. In [248], Zhang and Moayeri propose a purely theoretical model that assumes a regular city grid and predicts a single reflected path (around corners) and a constant adjustment for other multipath effects. Different calculations are used based on whether the receiver is on a neighboring street or a side (perpendicular) street. In [202], Rustako *et al.* suggest that only 6 rays are necessary for modeling line-of-sight links in urban street-canyons. In [117], Kanatas *et al.* suggest a simple two-dimensional ray-tracing model that assumes a uniform rectilinear building/street layout and makes a minimal validation against measurements. In [198], Rizk *et al.* propose a two-dimensional ray-tracing approach that can deal with arbitrary building layouts and go to some effort to validate their approach. In [176], Piazzi *et al.* evaluate a two-dimensional ray-tracing approach in a residental environment and find decent results when the transmitter is positioned above the rooftops. In [80], the authors extend the Walfisch-Ikegami model to include corrections from ray-tracing and static adjustments for the presence of trees.

More recently, authors have proposed three-dimensional models that require substantially more computation. In [241], Wölfle *et al.* propose a three-dimensional ray-optical model that utilizes substantial preprocessing to improve performance, as well as using the COST-231 model for LOS links. In [234] the same authors propose heuristics to simplify the computational complexity of prediction by only calculating the most important ("dominant") paths. In [211], Sridhara *et al.* propose a ray-tracing approach, but only claim that its accuracy is sufficient for simulation (and not prediction). Finally, [105] provides a survey of various ray-tracing approaches. In addition to those papers published in the academic literature, there are also a number of commercial planning systems that provide similar prediction tools (e.g., [189, 239, 51]). The Remcom Wireless Insight software [189], for instance, packages a number of popular path loss prediction models discussed above with their own three-dimensional ray-tracing system.

The majority of recent work in this area is concerned with optimization and preprocessing to make feasible the intractable number of calculations required for this approach. Although in some ways these models are the most advanced of all the models on the table, they are not useful in practice for accuracy-sensitive coverage mapping because of their large computation and data requirements. Computing the many path loss estimates required to generate a coverage map for a large urban area in a reasonable amount of

time is simply outside the abilities of the current models. Those models that can compute results quickly do so by selecting a relatively small subset of rays to model, which may or may not be the most important. Precise two- and three-dimensional environmental vector data is seldom available, becomes stale quickly, and is often costly even when it is available. When this data is available, it is not clear which attributes are most important—in many scenarios, building materials (and their conductivity and permittivity properties) must also be known to make accurate predictions. In short, while these models offer a great deal of promise, there is still much work needed to understand their accuracy, and reduce the cost associated with their use (both in terms of time and data acquisition). In particular, developing an understanding of the relationship between the performance of these models to the fidelity of their input data is essential.

2.3 Modeling With Measurements

All of the preceding models discussed are *a priori*. They make predictions about a given network and a given environment either using analytical expectations about propagation or empirical models collected from a different (but hopefully similar) environment, or some combination thereof. The final category of models are those whose design is based on the assumption that there is no single set of *a priori* constants, functions, or data that allow for sufficient description of a new environment with sufficient accuracy. These models assume that the burden of making some number of measurements is unavoidable. In a sense, these are more than models—they define a method for collecting measurements (sampling strategy) and a means of predicting (interpolating) the values at locations that have not been measured.

The seminal work in this area is by W.C. Lee in [132]. In this work, Lee proposes a theoretically justified methodology for averaging signal strength. He suggests that a mobile receiver should make measurements in arcs at varying distances from the transmitter. He argues that measurements within 20 to 40 wavelengths of one another should be averaged to obtain a central tendency and that an appropriate sample size is at minimum, 36 measurements. For 2.4 GHz, this works out to between 0.625 and 1.25 m, which is in agreement with a study made by Shin, 25 years after Lee's original publication [208]. In this work, Shin does a measurement study of Institute of Electrical and Electronics Engineers (IEEE) 802.11b/g networks, attempting to model signal strength variation over small distances. He finds that the wideband modulation

schemes used in 802.11g result in some immunity to fast fading effects, and that small scale variations are "averaged out" within a radius of approximately 1 wavelength (3.1 mm for 2.4 GHz). He discovers that measurements have a strong spatial correlation within $\approx$ 1 m and become uncorrelated at larger distances. In [131] and [133], Lee expands his original measurement based work into a general purpose fitted model that is still commonly used in planning cellular networks.

In [73], Evans *et al.* utilize Lee's proposals to model the propagation of a transmitter at 1.9 GHz and find that they are able to achieve approximately 9 dB Root Mean Square Error (RMSE). A similar approach was also taken in [143], where Medeisis and Kajackas fit measurements to the Hata model and do some investigation of the number of measurements needed to sufficiently correct the model and appropriate measurement methods. They find that in their environment 15-20 measurements are needed to tune the model sufficiently, and that measurements are most useful when taken in clusters along a path. In [60] the authors explicitly fit measurements in their environment but fail to show significant improvement over *a priori* predictions (achieving, on average, 9 dB RMSE no matter the approach).

2.3.1 Explicit Mapping

Hills carried out some of the early high level work on formalizing wireless planning in his attempts to design a network for Carnegie Mellon University [95]. Based on his experiences, he would go on to develop a measurement apparatus for doing on-the-fly mapping of indoor propagation to aid in network planning [96]. The network engineer must place a temporary transmitter and roll the cart around collecting measurements. The cart counts wheel rotations to determine position and orientation within a building. The software on the cart plots signal strength measurements and can make suggestions about channel assignment to minimize interference with neighboring networks. In [76], Fretzagias and Papadopouli suggest a method for mapping indoor environments where the total area is divided into grid cells. A large number of nodes are used to sound the channel and make measurements. Then the measurements from each node are used in tournament/voting fashion to determine the average signal at each grid cell.

2.3.2 Partition Models

The next group of models worth describing are "partition based" models, where measurements are taken in an environment where the key obstructions are identified (i.e., walls, trees, buildings, etc.). In this approach, measurements are taken and static path loss values are fitted for each obstruction. Once the model is bootstrapped with these fits, it can be used (in theory) in other environments. An early example of this approach is in the very nice work by Durgin *et al.* in [64], where the authors study path loss in a suburban environment at 5.8 GHz. Naturally, this approach extends easily to indoor environments where there are a large number of explicit obstacles (walls). This approach has been investigated much more thoroughly by Rappaport and colleagues at various frequencies [205, 24]. In [249], Zvanovec *et al.* propose a similar model. However, due to the lack of substantive quantitative analysis in this paper it is difficult to draw strong conclusions from the results. In [243], Xiang *et al.* propose another partition-based model that also gives some attention to sampling. They propose a "lazy sampling" algorithm that greedily selects transmitter locations. A receiver is then used to make measurements on a regular grid and the measurements are used to train a partition model. The authors show that this approach can produce an interpolated coverage map with approximately 6 dB residual error.

2.3.3 Iterative Heuristic Refinement

The most recent active measurement model is that of Robinson *et al.* in [200]. In this work, the authors attempt to identify coverage holes in large wireless networks. They study the Technology For All (TFA) network operated by Rice and the Google WiFi network in Mountain View, California. Robinson's approach combines an *a priori* model with a fitted partition model and then uses a push-pull heuristic to make corrections from measurements. For a given Access Point (AP) node (n), and a given point (p), the SNR is predicted by:

$$P_{dB}(p,n) = P_0 - 10\alpha log\left(\frac{d(n,p)}{d_0}\right) + \beta(n,p) \tag{2.89}$$

where P_0 is the transmitter EIRP, $d(n,p)$ is distance from the point to the node, α is the path loss exponent,

d_0 is the reference distance, and $\beta(n, p)$ is a fitted offset function. Omitting the offset function, this equation is identical to equation 2.11 in section 2.2.1.2. The offset function makes use of a vector data terrain map that describes the types of buildings between an AP and each possible receiver site (pixel). A training phase determines the path loss per unit distance for each building type, which then informs the offset function:

$$\beta(n, p) = \sum_{f \in F} C_f \times w(n, p, f) \tag{2.90}$$

where $f \in F$ are the terrain "features" on the LOS path between the node n and point p, C_f is the fitted weight (i.e., path loss per unit distance) of the feature type f and $w(n, p, f)$ is the length of intersection between this feature and the line-of-sight path between n and p.

In Robinson's proposal, sufficient "pilot" measurements are made to determine the C_f values for all f and the environment wide α is determined. Then, this model is used to predict the signal strength of each AP to a large number of equally spaced points around the node. A coverage metric must be defined (e.g., $SNR > 20$), which says where a point is "covered" or not. By applying this metric to the predictions around the radius of a node the range of the node as a function of the azimuth angle is obtained. Robinson fits a step function to this curve and uses the number of segments in the fitted step function to create a "segmented" coverage prediction of each node with a relatively small number of segments. Figures 2.7 and 2.8 show an example of this sectorization and fitting.

The remainder of Robinson's method, involves iterative refinement. A measurement is made as close to each coverage boundary as possible and then the boundary is pushed or pulled by a constant amount. This process is repeated until the push/pull amount is less than some threshold (Robinson suggests 3 dB, which seems reasonable based on prior studies of expected repeated measures variance, e.g., [198]).

2.3.4 Active Learning and Geostatistics

As a generalization of the iterative refinement approach described above, the machine learning literature offers an approach called "active learning". In active learning systems, an algorithm is able to choose its training data, as opposed to passively trained systems that must learn a behavior from a set of "random" observations.

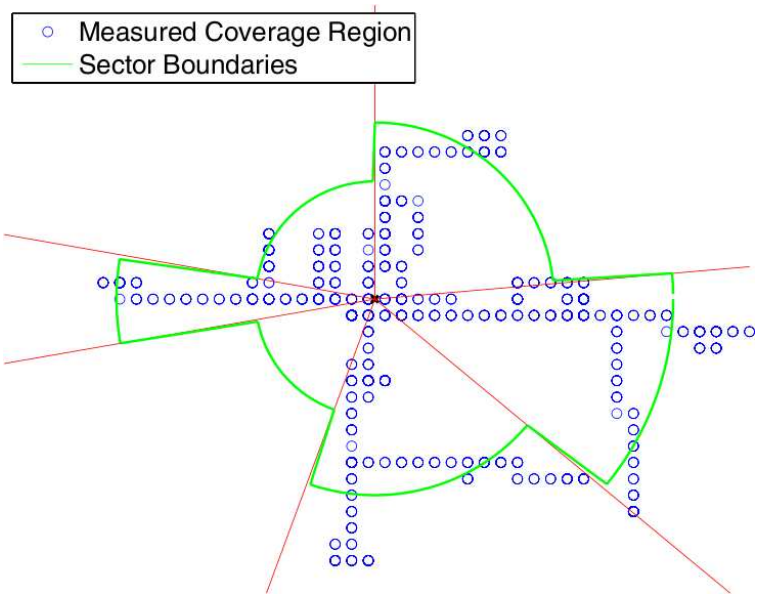

Figure 2.7: Example of sectorized propagation model for a single transmitter using the Robinson model. The measured (oracle) coverage is given as blue circles. The predicted/fitted coverage is given as sector boundaries that are adjusted (pushed and pulled) by additional measurements. Figure taken from [200].

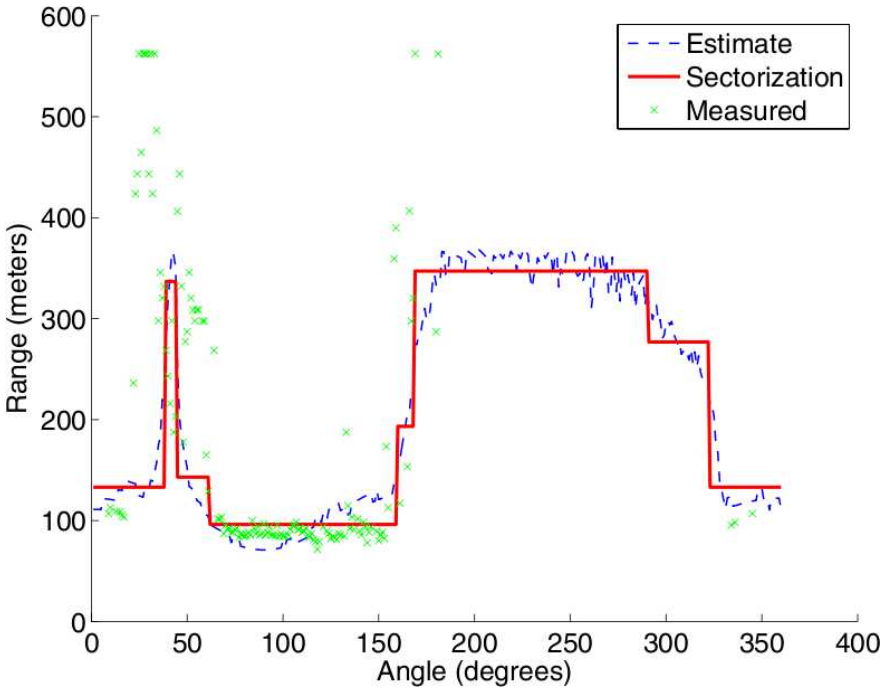

Figure 2.8: Example of fitted step function to measurements for the Robinson method. Figure taken from [200].

In [49], Cohn *et al.* provide a summary of this area, deriving active learning approaches to three kinds of learning systems: neural networks, mixed Gaussians, and locally weighted regression. Additional training data (samples) are chosen to minimize model variance. Cohn shows that active learning approaches far outperform randomly selected training data for training a model to solve the arm kinematics problem[2] .

Active learning has an analogous problem in the realm of geostatistics (and typically applied in ecological soil sampling) termed "optimized sampling" [230, 139]. In this version of the problem, additional data for a trained model is selected by minimizing some metric of variance (Kriging variance is generally used in geostatistical treatments). Regardless of the domain from which it is drawn, the task is fundamental: given some existing model, can we chose the next set of measurements that most improves the accuracy of the model itself?

2.4 Comparative Studies

The vast majority of existing work analyzing the efficacy of path loss models has been carried out by those authors who are proposing their own improved algorithm. In such cases, the authors often collect data in an environment of interest and then show that their model is better able to describe this data than one or two competing models. Unfortunately, this data is rarely published to the community, which makes comparative evaluations impossible. One noteworthy exception is the work of the COST-231 group in the early 1990's, which published a benchmark data set (900 MHz measurements taken in European cities) and produced a number of competing models that were well performing with respect to this reference [48]. This effort produced a number of well validated models that are tuned for 900 MHz transmitters in urban environments.

Similarly, there was substantial work done in the US, Japan, and several other countries in the 1960s and 1970s to come up with accurate models for predicting the propagation of analog TV signals (e.g., [57]). This flurry of work produced many of the models that are still used today in network simulators and wireless planning tools: the ITM [98], the Egli Model [69], and the Hata-Okumura model [157], to name a few. However, it is unclear what the implications are of using these models, which were created for use in a

[2] In the arm kinematics problem, a trained model attempts to predict the tip position of a robotic arm given a set of joint angles.

specific domain, to make predictions about another domain.

There are several works that compare a number of models with respect to some data. In [62], the authors compare five models with respect to data collected in rural and suburban environments with a mobile receiver at 910 MHz. They discuss the abilities of each model, but abstain from picking a winner. In [19], the authors compare three popular models to measurements collected at 3.5 GHz by comparing a least squares fit of measurements to model predictions. The authors highlight the best of the three, which turns out to be the ECC-33 model proposed in [72]. In [207], Sharma *et al.* do a very similar analysis, but instead focus on measurements made in India at 900 and 1800 MHz. In contrast to [19], they find that the Stanford University Interim model (SUI) and COST-231 models perform best.

2.5 Discussion

Making sense of the vast and varied landscape of path loss models can be a precarious task for the uninitiated researcher. In this chapter, a new taxonomy for reasoning about commonalities between these models was described. In terms of functionality and intent, the models can be further categorizd into classes based on those that are appropriate for (a) coverage and radio environment mapping, (b) rough planning, and (c) simulation. Applications that require accurate maps of the radio environment are probably best suited for an active measurement method that can resolve predictions with directed measurements. When it is not possible to make measurements of the environment directly, an experimenter must accept some (possibly substantial) error. Many-ray methods are promising, but their accuracy is intimately tied to the accuracy of data describing the environment and obstacles, which is seldom available at a useful resolution and can be very costly to collect and update. These models are also famously slow, requiring a substantial amount of computation for even a few predictions. Those looking to path loss models for rough planning are able to choose amongst dozens of seemingly similar proposals, accepting the caveat that it is impossible to verify accuracy. For this reason, the most-heavily used standard models are recommended for the sake of comparability (i.e., Okumura-Hata, Longley-Rice ITM, etc.). Simulations have similar needs to rough planning applications, except they also require the prediction of a distribution of reasonable values around the median for repeated-measured/Monte Carlo techniques. Hence, stochastic basic models (or deterministic

models with a stochastic fading parameter) are likely the most suitable, and there are several to chose from. Again, there is value in choosing amongst the most well-known, standard models (e.g., Hata with lognormal fading, or the recent Herring model).

Although there are many possible directions for future work in this area, measurement-based methods and rigorous (comparative) validation are most needed. Applications that make use of these models require an understanding of their real-world accuracy, and researchers need guidance in choosing amongst the many existing proposals. To this end, chapter 3 describes an important first step in this direction. Although this work will seek to provide a baseline performance for *a priori models*, more work is needed in general to resolve the imbalance between the quantity of models proposed and the extent to which they have been validated in practice.

Of all the models discussed so far, two extremes in terms of information requirements are apparant. On one end of the spectrum are basic models, like the Hata model, that require very little information about the environment—simply the link geometry and some notion of the general environmental category. At the other end are many-ray models which make use of vector data for obstacles to calculate specific interactions, requiring knowledge of the exact position and shape of all obstacles. In between these two extremes, there are very few models. Possible examples include the ITM and ITU-R 452 models, which make use of some additional information from public geographic datasets. A natural question then, is whether there is some other source of data available that could be used to inform better predictions, but is not as costly or difficult to obtain as detailed vector data. For instance: models that make use of high resolution satellite orthoimagery and machine vision techniques, a high resolution Digital Surface Model (DSM) (where surface clutter is not "smoothed away" as it is in digital elevation/terrain models, e.g., [103]), "crowd-sourced" building vector data *vis a vis* Google Sketchup [14], or topographic and zoning maps (e.g., [200]). So far, this data-mining approach to prediction, although promising, has seen little rigorous investigation.

There is simply no better way to generate truthful predictions than to start with ground-truth itself. For this reason, this thesis argues that the future of wireless path loss prediction methods will be active measurement designs that attempt to extract information from directed measurements. In particular, geostatistical approaches that favor robust sampling designs and explicitly model the spatial structure of measure-

ments are promising (e.g., [119, 236]). General machine learning approaches, and active learning strategies may also be fruitful, but applying those methods to the domain of path loss modeling and coverage mapping is currently unexplored. Future work in this area is likely to focus on refining sampling and learning strategies using measurement based methods, as well as extracting as much information as possible from existing sources using data mining. Methods for parallelizing computation and preprocessing datasets are also needed to make predictions quickly (this is especially true when these models are used in real time applications). And, once predictions are made, efficient storage and querying of these spatial databases is an opportune area for further work.

As the the prevalence and importance of wireless networks continues to grow, so too will the need for better methods of modeling and measuring wireless signal propagation. This chapter has given a broad overview of approaches to solving this problem proposed in the last 60 years. Most of this work has been dominated by models that extend on the basic electromagnetic principles of attenuation with theoretical and empirical corrections. More recently, work has focused on developing complex theoretical deterministic models. It is likely that the next generation of models will be data-centric, deriving insight from directed measurements and possibly using hybridized prediction techniques, such as the geostatistical approach described in this thesis. Regardless of the approach that is taken, there is substantial possibility for future work in this area, with the promise of great impact in many crucial applications.